

Transition energies of atomic lawrencium

A. Borschevsky¹, E. Eliav¹, M.J. Vilkas², Y. Ishikawa², and U. Kaldor^{1,a}

¹ School of Chemistry, Tel Aviv University, 69978 Tel Aviv, Israel

² Department of Chemistry, University of Puerto Rico, P.O. Box 23346, San Juan, Puerto Rico 00931–3346, USA

Received 22 November 2006 / Received in final form 11 February 2007

Published online 23 March 2007 – © EDP Sciences, Società Italiana di Fisica, Springer-Verlag 2007

Abstract. Transition energies of the superheavy element lawrencium, including the ionization potential, excitation energies and electron affinities, are calculated by the intermediate Hamiltonian coupled cluster method. A large basis set ($37s31p26d21f16g11h6i$) is used, as well as an extensive P space ($6s5p4d2f1g$). The outer 43 electrons are correlated. Accuracy is monitored by applying the same approach to lutetium, the lighter homologue of Lr, and comparing with experimentally known energies. QED corrections are included. The main goal is to predict excitation energies, in anticipation of planned spectroscopy of Lr. The ground state of Lr is $7s^27p^2P_{1/2}$, unlike the $5d6s^2^2D_{3/2}$ of Lu. Predicted Lr excitations with large transition moments in the prime range for the planned experiment, 20 000–30 000 cm^{-1} , are $7p \rightarrow 8s$ at 20 100 cm^{-1} and $7p \rightarrow 7d$ at 28 100 cm^{-1} . The average absolute error of 20 excitation energies of Lu is 423 cm^{-1} , and the error limits for Lr are put at 700 cm^{-1} . The two electron affinities measured recently for Lu are reproduced within 55 cm^{-1} , and a third bound state of Lu^- is predicted.

PACS. 32.30.-r Atomic spectra – 31.30.Jv Relativistic and quantum electrodynamic effects in atoms and molecules – 31.15.Dv Coupled-cluster theory

1 Introduction

The spectroscopic study of superheavy atoms ($Z \gtrsim 100$) presents a severe challenge to the experimentalist. While certain chemical properties of these elements may be elucidated in single-atom experiments [1,2], spectra can be measured only in sizable samples. The first such study of a superheavy atom [3] used 2.7×10^{10} atoms of ^{255}Fm with a half life of 20.1 h, long enough to make possible shipment of the sample from Oak Ridge, Tennessee, where it was produced, to the Max-Planck-Institut für Kernphysik in Heidelberg, where the spectrum was taken. Spectroscopic measurements are currently planned for No and Lr, which have shorter lifetimes, by a collaboration based at GSI [4], with production and measurement taking place in the same institute. Such measurements must be accompanied by high-level calculations. The low production rates of the atoms in nuclear fusion reactions, below 10 per second, and short lifetimes, on the order of seconds, necessitate reliable prediction of the position of transition lines, to avoid the need for broad wavelength scans. In addition, theoretical studies are crucial for identifying the lines. Indeed, the Fm measurements [3] were accompanied and guided by multiconfiguration Dirac-Fock (MCDF) calculations. The purpose of the present work is to provide sufficiently accurate transition energies for

the lawrencium atom. The accuracy of the prediction is estimated by applying the same method to lutetium, the lighter homologue of Lr, where experimental transition energies are available.

The coupled-cluster (CC) approach is probably the most powerful tool for high quality atomic and molecular calculations [5]. The Fock-space coupled-cluster (FSCC) scheme, a multireference variant of the CC method, has provided the most accurate transition energies for many atomic and molecular systems [6]. It takes account of non-dynamic electron correlation by the multiconfigurational approach, including the important electron configurations in the model (P) space, and at the same time provides a good description of dynamic correlation by incorporating many millions of excitations to Q space determinants. FSCC results are usually more accurate than MCDF values, since the latter method involves far fewer excitations, thus incorporating a smaller segment of Q and giving less extensive description of dynamic correlation. Thus, the FSCC error [7] for energy differences in the f^2 manifold of Pr^{3+} is four times smaller than that of MCDF [8]. Another example is the electron affinity (EA) of Tl, measured recently [9]. Before the experimental value was known, multireference configuration interaction [10] and MCDF [11] calculations predicted an EA of 0.27–0.29 eV, whereas FSCC [12] gave a significantly higher 0.40 eV. The measured 0.377(13) eV is in much better agreement with the latter value.

^a e-mail: kaldor@jade.tau.ac.il

The FSCC approach has been augmented and improved by the development of intermediate Hamiltonian Fock-space coupled cluster (IHFSCC) methods [13–16]. These make possible the use of much larger and more flexible P spaces without running into intruder states and divergence, thereby increasing the accuracy obtained [17–21]. Pilot applications with the extrapolated intermediate Hamiltonian approach [22, 23] reproduced the known ionization potentials and electron affinities of the alkali atoms within 1 meV.

The available experimental information on the levels of Lu appears in the compendium of Martin et al. [24]. A recent addition is the electron affinity of Lu, measured by Davis and Thompson [25]. Desclaux and Fricke [26], and, more recently, Zou and Fischer [27], calculated some transition energies of Lu and Lr using the MCDF approach. Other methods used include density functional theory (DFT) by Vosko et al. [28] and pseudopotential and DFT studies by Liu et al. [29]. The FSCC method was applied to many levels of the atoms [30]. Here we apply the intermediate Hamiltonian coupled cluster approach to the electronic spectra of the Lu and Lr atoms, compare the results to experimental values for Lu, and predict transition energies for lawrencium.

2 Method

The intermediate Hamiltonian (IH) approach was originally introduced by Malrieu [31] in the framework of degenerate perturbation theory. The model space P is partitioned into two parts, the main P_m and intermediate P_i , and an intermediate Hamiltonian H_I in P is derived, the eigenvalues of which give good approximation to the eigenvalues of H dominated by main model space components. The other eigenvalues, dominated by the intermediate (P_i) components, are arbitrary (in practice, the latter are also well reproduced in many cases). This flexibility was exploited by Malrieu to eliminate the influence of intruders on the convergence of the degenerate many-body perturbation theory expansion up to 3rd order. Conditions on problematic $P_i \rightarrow Q$ transitions, associated with small energy denominators and convergence difficulties, were derived, leading to equations similar to but not identical with the Bloch equation. We have derived several intermediate Hamiltonian approaches applicable in any order, including the all-order coupled-cluster method [13, 15, 23]. Our first IH formulation is used here. It is described briefly in this section; a more extensive description may be found in an earlier publication [13].

Three projection operators are used, satisfying

$$P_m + P_i = P, \quad P + Q = 1. \quad (1)$$

Two sets of wave-like operators are defined [31] and expanded in coupled-cluster normal-ordered exponential ansätze. $\Omega = 1 + \chi$ is a standard wave operator in P_m ,

$$\Omega P_m |\Psi_m\rangle = \{\exp S\} P_m |\Psi_m\rangle = |\Psi_m\rangle, \quad (2)$$

where $|\Psi_m\rangle$ denotes an eigenstate of the Hamiltonian H with the largest components in P_m , and $R = 1 + \Delta$ is an operator in P , satisfying

$$RP|\Psi_m\rangle = \{\exp T\}P|\Psi_m\rangle = |\Psi_m\rangle. \quad (3)$$

It should be noted that the last equation, and therefore all equations derived from it, applies when operating on $|\Psi_m\rangle$ but not necessarily on $|\Psi_i\rangle$. This feature distinguishes R from a bona fide wave operator. The cluster equation for S in the (n) sector of the Fock space is [17]

$$Q[S^{(n)}, H_0]P_m = Q(\overline{VQ_i\Omega} - \overline{\chi P_m V Q_i \Omega})^{(n)} P_m, \quad (4)$$

where $Q_i = 1 - P_i = Q + P_m$. No $P_i S P_m$ elements appear in the equation, so that P_i acts as a buffer between P_m and Q , facilitating convergence and avoiding intruder states. Equation (4) is valid provided $QSP_m \simeq QTP_m$, which is rather easy to achieve and is checked in the calculation. After (4) is solved for QSP_m , the equation for QTP is solved,

$$(E - H_0)QT^{(n)}P = Q(S(E - H_0)P_m + (\overline{VR}) - (\overline{\chi P_m VR}))^{(n)} P. \quad (5)$$

E is an arbitrary constant, chosen to facilitate convergence. Tests have shown that E may be changed within broad bounds (hundreds of Hartrees) with small effect (1 meV or less) on calculated transition energies. The final step is the construction of the intermediate Hamiltonian

$$H_I = PHRP, \quad (6)$$

which gives upon diagonalization the correlated energies of $|\Psi_m\rangle$,

$$H_I P |\Psi_m\rangle = E_m P |\Psi_m\rangle. \quad (7)$$

The dimension of the H_I matrix is that of P ; however, only the eigenvalues corresponding to $|\Psi_m\rangle$ are required to satisfy equation (7). The other eigenvalues, which correspond to states $|\Psi_i\rangle$ with the largest components in P_i , may include larger errors.

The Lamb shifts were estimated for each state by evaluating the electron self-energy and vacuum polarization using the approximation scheme of Indelicato et al. [32]. The code described in references [32, 33] was adapted to our basis set expansion procedure by Vilkas and Ishikawa [34]. All the necessary radial integrals were evaluated analytically. In this scheme [33], the screening of the self energy is estimated by integrating the charge density of a spinor to a short distance from the origin, typically 0.3 Compton wavelengths. The ratio of the integral computed with a spinor and that obtained from the corresponding hydrogenic spinor is used to scale the self-energy correction for a bare nuclear charge that has been computed by Mohr [35]. Extensive relativistic configuration interaction (RCI) wave functions were used. While the IHFSCC excitation energies are expected to be more accurate, the RCI functions reproduced them in most cases within a few percent, so that the QED corrections should be quite accurate. The RCI functions were also used to obtain transition amplitudes to the Lr ground state.

Table 1. Transition energies of Lu (cm^{-1}).

Method Ref.	Expt. [24,25]	IHFSCC present	+QED present	FSCC [30]	MCDF [27]	DFT [28]
Ionization potential						
$5d6s^2$ $^2D_{3/2}$	43 762	42 836		42 757		44 504 42 858
Excitation energies						
$5d6s^2$ $^2D_{5/2}$	1994	1945	1947	1975		1580 1536
$6s^26p$ $^2D_{P_{1/2}}$	4136	4080	4082	3828	4186	3862 3094
		7476	7383	7390	7140	7462
$6s^27s$ $^2S_{1/2}$	24 126	23 730	23 745			
$6s^27p$ $^2P_{1/2}$	29 430	30 457	30 459			
		30 489	30 930	30 934		
$6s^26d$ $^2D_{3/2}$	31 542	31 929	31 933			
		31 714	32 040	32 041		
$6s^28s$ $^2S_{1/2}$	34 610	33 978	33 969			
$6s^25f$ $^2F_{5/2}$	36 633	36 595	36 593			
		36 644	36 595	36 593		
$6s^28p$ $^2P_{1/2}$	36 809	36 005	35 980			
		37 131	36 119	36 094		
$6s^29s$ $^2S_{1/2}$	38 458	37 520	37 554			
$6s^27d$ $^2D_{3/2}$	36 769	37 028	37 005			
		36 953	37 106	37 090		
$6s^29p$ $^2P_{1/2}$	39 321	39 554				
		39 424	39 861			
$6s^210s$ $^2S_{1/2}$	40 282	39 318				
$6s^211s$ $^2S_{1/2}$	41 120	40 956				
Electron affinities						
$6s^26p5d^3F_2$	2742	2706		2076		4258 2173
$6s^26p^2$ 3P_0	1290	1345		746		
$6s^26p5d^3D_2$		917		-336		

3 Application

The Dirac-Coulomb-Breit Hamiltonian serves as the framework for the calculations. The Dirac-Fock-Breit orbitals are first obtained, and correlation is included at the coupled cluster singles-and-doubles (CCSD) level. The closed-shell reference states for the Lu and Lr atoms are the monocations (Xe) $4f^{14}6s^2$ and (Rn) $5f^{14}7s^2$, respectively. The states of the neutral atoms are reached by adding an electron to the reference determinants in a set of valence orbitals, and the anions are obtained by adding a second electron. Valence orbitals are added to the P_m and P_i spaces until the resulting transition energies converge. For Lu, P_m comprised $2s1p1d$ orbitals (the lowest orbitals of each l not occupied in the reference closed-shell determinant of Lu^+), and the total P included $5s4p3d1f$ orbitals. Somewhat larger model spaces were needed for Lr, with $2s2p2d$ in P_m and $6s5p4d2f1g$ in P . Note that P orbitals include those in P_m .

The universal basis set [36] is used, consisting of even tempered Gaussian-type orbitals with exponents given by

$$\zeta_n = \gamma \times \delta^{(n-1)}, \quad \gamma = 106\,111\,395.371\,615, \\ \delta = 0.486\,752\,256\,286. \quad (8)$$

The basis set was increased until transition energies converged. The basis used for both atoms includes 37 s functions ($n = 1-37$), 31 p ($n = 5-35$), 26 d ($n = 9-34$), 21 f ($n = 13-33$), 16 g ($n = 17-32$), 11 h ($n = 21-31$), and 6 i orbitals ($n = 25-30$). The basis functions are left uncontracted. Virtual atomic orbitals with energies higher than 200 Hartrees are discarded. The outer 43 electrons of the atoms were correlated, leaving out the 28 inner electrons of Lu and 60 inner electrons of Lr after the Dirac-Coulomb-Breit stage.

4 Results and discussion

Since many transition energies of the lanthanide Lu are known with high accuracy [24,25], their calculation provides a check on the accuracy of the method and the validity of predictions for the actinide Lr. The results for the lighter element are presented and compared with experiment and previous computations in Table 1. Very good accuracy is obtained, with an average error of 423 cm^{-1} or 0.05 eV for the twenty excitation energies shown. The QED corrections are small. The two electron affinities measured recently by Davis and Thompson [25] are reproduced within 7 meV, and an additional bound state

Table 2. IHFSCC transition energies of Lr (cm^{-1}).

State		+QED	
Ionization potential			
$7s^27p$	$^2P_{1/2}$	39 466	39 469
Excitation energies			
$6d7s^2$	$^2D_{3/2}$	1436	1408
	$^2D_{5/2}$	5106	5082
$7s^27p$	$^2P_{3/2}$	8413	8389
$7s^28s$	$^2S_{1/2}$	20 118	20 131
$7s^28p$	$^2P_{1/2}$	26 111	26 104
	$^2P_{3/2}$	27 508	27 491
$7s^27d$	$^2D_{3/2}$	28 118	28 096
	$^2D_{5/2}$	28 385	28 380
$7s^29s$	$^2S_{1/2}$	30 119	30 113
$7s^29p$	$^2P_{1/2}$	32 295	32 290
	$^2P_{3/2}$	32 840	32 841
$7s^26f$	$^2F_{5/2}$	32 949	32 933
	$^2F_{7/2}$	32 950	32 961
$7s^28d$	$^2D_{3/2}$	33 473	33 458
	$^2D_{5/2}$	33 635	33 626
$7s^210s$	$^2S_{1/2}$	33 942	
Electron affinities			
$7s^27p^2$	3P_0	3828	3838
$7s^27p6d$	3F_2	1161	1155

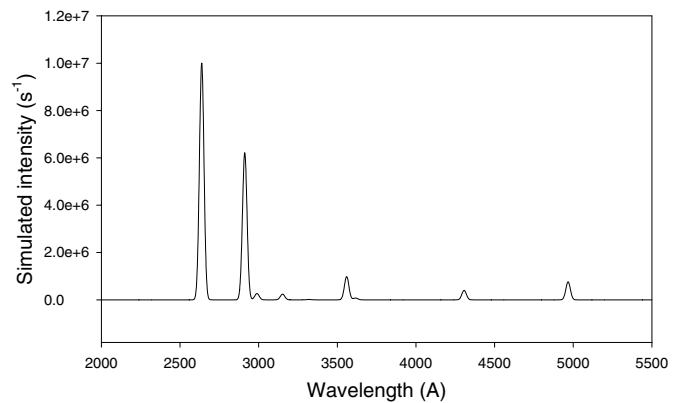
of the anion is predicted. DFT values are quite far from experiment.

Table 2 shows the transition energies of lawrencium. Note that the ground state ($7s^27p \ ^2P_{1/2}$) is different from that of lutetium ($6s^25d \ ^2D_{3/2}$), as relativity pushes the $7p$ orbital below the $6d$. The QED corrections to the transition energies are small, below 30 cm^{-1} . This small contribution reflects the fact that the $7s$ population does not change for the transitions reported. Some excitations involving holes in the $7s$ shell were calculated by the RCI method; they exhibit larger QED effects, between $200\text{--}400 \text{ cm}^{-1}$. The prime region for observing transitions in the planned GSI experiment is between $20\,000$ and $30\,000 \text{ cm}^{-1}$. Our calculations predict several excitations with large transition amplitudes in this region. The strongest lines in the range of the experiment will correspond to $7p \rightarrow 8s$ at $20\,100 \text{ cm}^{-1}$ and $7p \rightarrow 7d$ at $28\,100 \text{ cm}^{-1}$. The $7p \rightarrow 9s$ transition at $30\,100 \text{ cm}^{-1}$ is also dipole allowed, but the very different spatial distribution of the two orbitals is expected to make it weaker than the other two. Other states in the same energy range come from the $6d7s7p$ configuration. These were not calculated here, and are expected to carry small transition amplitudes because of the parity selection rule. Note that the only previous accurate calculation of Lr excitation energies [27] treated just the lowest transition, $7s \rightarrow 6d_{3/2}$, which is in the infrared region and not subject to the planned experiment.

Transition amplitudes cannot be obtained by the current FSCC programs, and the RCI method was therefore used to compute them. The transition amplitudes

Table 3. RCI amplitudes of E1 transitions to the $7s^27p_{1/2}$ ground state of Lr. The upper levels are designated by the dominant electron configurations; other configurations may contribute substantially.

λ (Å)	Upper level	J	A (s^{-1})
2637.7	$6d_{3/2}6d_{5/2}7s$	1/2	3.6×10^8
2911.3	$6d_{5/2}^27s$	3/2	2.2×10^8
2988.9	$7s^28d_{3/2}$	3/2	9.4×10^6
3151.8	$6d_{3/2}^27s$	3/2	8.6×10^6
3319.5	$7s^29s$	1/2	6.0×10^5
3559.2	$7s^27d_{3/2}$	3/2	3.5×10^7
3616.2	$7s7p_{1/2}7p_{3/2}$	1/2	2.7×10^6
4306.4	$7s7p_{1/2}^2$	1/2	1.4×10^7
4967.5	$7s^28s$	1/2	2.7×10^7

**Fig. 1.** Simulated E1 spectrum of Lr.

are shown in Table 3. Note that some excited states, in particular those with a single $7s$ electron, have large contributions from several configurations. Thus, the first two states in Table 3 have RCI coefficients between $0.4\text{--}0.5$ for each of the $7s7p_{1/2}7p_{3/2}$, $6d_{3/2}6d_{5/2}7s$, and $7s6d_{5/2}^2$ configurations, and their assignment is somewhat arbitrary. The simulated spectrum, obtained by convolution with a Gaussian function with 20 Å full width at half maximum, is shown in Figure 1. As noted above, the RCI method gave excitation energies within a few hundred wavenumbers of FSCC values in most cases. Some states, such as the $7s^26d$ levels, showed much larger differences (several thousand cm^{-1}). The two states with the largest RCI transition amplitudes are outside the range of the planned experiment. They are dominated by the $6d^27s$ and $7s7p^2$ configurations, which cannot at present be included in the P space. Consequently, these states do not appear in the FSCC calculations, and their energies may have larger errors than states obtained by FSCC. The transitions at $20\,100$ and $28\,100 \text{ cm}^{-1}$ carry the next highest amplitudes, and are the most likely to be observed.

5 Summary and conclusion

Excitation energies of Lr are calculated, in anticipation of planned spectroscopy of this superheavy element. The intermediate Hamiltonian coupled cluster method applied, as well as other aspects of the implementation (basis sets, number of electrons correlated, structure of P spaces), are tested by application to Lu, the lighter homologue of Lr. Dipole allowed transitions falling in the 20 000–30 000 cm^{-1} range and expected to have large amplitude are $7s^27p\ ^2P_{1/2} \rightarrow 7s^28s\ ^2S_{1/2}$ at 20 100 cm^{-1} and $7s^27p\ ^2P_{1/2} \rightarrow 7s^27d\ ^2D_{3/2}$ at 28 100 cm^{-1} . The average absolute error of calculated Lu transition energies is 423 cm^{-1} ; a conservative estimate of the error bound in Lr is 700 cm^{-1} .

Nobelium is another superheavy candidate for spectroscopic measurements in the near future. Similar applications to its spectrum (and to Yb, its lighter homologue) are in progress.

This research was supported by the US-Israel Binational Science Foundation and by the Israel Science Foundation.

References

1. *The Chemistry of Superheavy Elements*, edited by M. Schädel (Kluwer Academic Publishers, Dordrecht, 2003)
2. V. Pershina, D.C. Hoffman, in *Theoretical Chemistry and Physics of Heavy, Superheavy Elements* (Kluwer Academic Publishers, Dordrecht, 2003), p. 55
3. M. Sewtz, H. Backe, A. Dretzke, G. Kube, W. Lauth, P. Schwamb, K. Eberhardt, C. Grüning, P. Thörle, N. Trautmann, P. Kunz, J. Lassen, G. Passler, C.Z. Dong, S. Fritzsche, R.G. Haire, *Phys. Rev. Lett.* **90**, 163002 (2003)
4. Backe et al., *Eur. Phys. J. D* **45**, 99 (2007)
5. For a recent review see R.J. Bartlett, in *Modern Electronic Structure Theory*, edited by D.R. Yarkony (World scientific, Singapore, 1995), Vol. 2, p. 1047
6. For a review on multireference CC methods, particularly the FSCC approach, see D. Mukherjee, S. Pal, *Adv. Quantum Chem.* **20**, 292 (1989); for a review on non-relativistic FSCC applications see U. Kaldor, *Theor. Chim. Acta* **80**, 427 (1991); for a review on relativistic FSCC applications see U. Kaldor, E. Eliav, *Adv. Quantum Chem.* **31**, 313 (1998)
7. E. Eliav, U. Kaldor, Y. Ishikawa, *Phys. Rev. A* **51**, 225 (1995)
8. Z. Cai, V. Meiser Umar, C. Froese Fischer, *Phys. Rev. Lett.* **68**, 297 (1992)
9. D.L. Carpenter, A.M. Covington, J.S. Thompson, *Phys. Rev. A* **61**, 042501 (2000)
10. A. Ferran, F. Moto, J. Novoa, *Chem. Phys.* **166**, 77 (1992)
11. W.P. Wijesundera, *Phys. Rev. A* **55**, 1785 (1997)
12. E. Eliav, Y. Ishikawa, P. Pyykkö, U. Kaldor, *Phys. Rev. A* **56**, 4532 (1997)
13. A. Landau, E. Eliav, U. Kaldor, *Chem. Phys. Lett.* **313**, 399 (1999)
14. A. Landau, E. Eliav, U. Kaldor, *Adv. Quantum Chem.* **39**, 171 (2001)
15. A. Landau, E. Eliav, Y. Ishikawa, U. Kaldor, *J. Chem. Phys.* **121**, 6634 (2004)
16. U. Kaldor, E. Eliav, A. Landau, in *Fundamental World of Quantum Chemistry*, edited by E.J. Brandas, E.S. Kryachko (Kluwer, 2004), Vol. III, pp. 365–406
17. A. Landau, E. Eliav, Y. Ishikawa, U. Kaldor, *J. Chem. Phys.* **113**, 9905 (2000)
18. A. Landau, E. Eliav, Y. Ishikawa, U. Kaldor, *J. Chem. Phys.* **115**, 6862 (2001)
19. A. Landau, E. Eliav, Y. Ishikawa, U. Kaldor, *J. Chem. Phys.* **114**, 2977 (2001)
20. A. Landau, E. Eliav, Y. Ishikawa, U. Kaldor, *J. Chem. Phys.* **115**, 2389 (2001)
21. E. Eliav, A. Landau, Y. Ishikawa, U. Kaldor, *J. Phys. B* **35**, 1693 (2002)
22. E. Eliav, M.J. Vilkas, Y. Ishikawa, U. Kaldor, *Chem. Phys.* **311**, 163 (2005)
23. E. Eliav, M.J. Vilkas, Y. Ishikawa, U. Kaldor, *J. Chem. Phys.* **122**, 224113 (2005)
24. W.C. Martin, R. Zalubas, L. Hagan, *Atomic Energy Levels — The Rare-Earth Elements*, US Natl. Bur. Stand. Ref. Data Ser., US Natl. Bur. Stand. Circ. No. NBS 60 (US GPO, Washington, DC, 1978); <http://physics.nist.gov/PhysRefData/Handbook/>
25. V.T. Davis, J.S. Thompson, *J. Phys. B* **34**, L433 (2001)
26. J.-P. Desclaux, B. Fricke, *J. Phys.* **41**, 943 (1980)
27. Y. Zou, C.F. Fischer, *Phys. Rev. Lett.* **88**, 183001 (2002)
28. S.H. Vosko, J.A. Chevary, *J. Phys. B* **26**, 873 (1993)
29. W. Liu, W. Küchle, M. Dolg, *Phys. Rev. A* **58**, 1103 (1998)
30. E. Eliav, U. Kaldor, Y. Ishikawa, *Phys. Rev. A* **52**, 291 (1995)
31. J.-P. Malrieu, Ph. Durand, J.-P. Daudey, *J. Phys. A* **18**, 809 (1985)
32. P. Indelicato, O. Gorceix, J.P. Desclaux, *J. Phys. B* **20**, 651 (1987)
33. Y.-K. Kim, in *Atomic Processes in Plasmas*, edited by Y.-K. Kim, R.C. Elton, *AIP Conf. Proc.* **206** (AIP, New York, 1990), p. 19
34. M.J. Vilkas, Y. Ishikawa, *Phys. Rev. A* **68**, 012503 (2003); M.J. Vilkas, Y. Ishikawa, *J. Phys. B* **37**, 1803 (2004)
35. P.J. Mohr, *Phys. Rev. A* **46**, 4421 (1992)
36. G.L. Malli, A.B.F. Da Silva, Y. Ishikawa, *Phys. Rev. A* **47**, 143 (1993)